

## RESEARCH ARTICLE

# New constant-velocity component paths for objects moving in vertical space

M. Pakdemirli\*

Department of Mechanical Engineering, Manisa Celal Bayar University, 45140, Muradiye, Yunusemre, Manisa, Turkey

Phone: +90(532)5678543

**ABSTRACT** - Paths of vehicles under restricted conditions are of technological interest in navigation engineering. One such restriction may be to fix one of the velocity components during motion. For objects moving in a two-dimensional vertical space, the differential equations determining the paths of the objects for which one of the velocity components remains constant are derived. First, the no thrust force case is investigated. The two paths in which the velocity components remain constant are determined by finding exact solutions of the associated differential equations. While the constant  $x$ -component case produces the well-known parabolic solution, the constant  $y$ -component case reveals a new solution called the 2/3 rule. Then, the differential equations for an object moving with constant  $x$  and  $y$  velocity components are derived separately for the constant-magnitude thrust force case. Since the equations inherit high nonlinearities, exact analytical solutions cannot be obtained for the constant-magnitude thrust force case. Instead, approximate solutions obtained by the Perturbation Iteration Method are compared with the Runge-Kutta numerical solutions. Within the range of validity, the approximate solutions can be employed to determine the path instead of the numerical solutions. The approximate analytical solutions would reduce the computational cost of integrating the original numerical solutions. The study may find applications in determining the paths of flying objects such as projectiles, rockets, and aerial vehicles.

**ARTICLE HISTORY**

Received : 25<sup>th</sup> Apr. 2024

Revised : 13<sup>th</sup> Aug. 2024

Accepted : 19<sup>th</sup> Sept. 2024

Published : 30<sup>th</sup> Sept. 2024

**KEYWORDS**

*Dynamics of motion*

*Thrust forces*

*Path equation*

*Ordinary differential equations*

*Perturbation iteration methods*

*Numerical solutions*

## 1. INTRODUCTION

Determining the paths of navigating objects under certain assumptions is of technological importance since either the paths can be employed in designing roads for land vehicles or they can be useful in determining the routes of aerial and marine vehicles. For paths in a horizontal two-dimensional space, parametric equations called ‘Clothoids’ are frequently used in designing the curved portions of highways [1-8]. Historical and basic information on Clothoids can be found in [7]. For control problems of clothoid-based navigation, it has been discussed in [8]. Alternative curves to clothoids were suggested, such as the quartic parabola, the blossom curve, and cosinusoid and sinusoid curves [9]. Using polynomials of high degrees, the shapes of railway entries and exits are optimized using control theory [10]. The aim is to smooth the transition from a straight path to a circular one. The curvature and arc length are linearly related to clothoidal curves. Since the normal component of acceleration, which leads to side slip and turnover incidents, does not remain constant for clothoidal curves, paths maintaining constant normal acceleration curves were proposed recently [11,12], which are safer to track in navigation. Determining path equations in vertical space is another technological task that has been found to have applications in determining the paths of aerial vehicles and land vehicles. Designing tracks for roller coasters is one potential area of research. Many methods have been employed for this task, such as the Cubic B-Spline method [13], Cubic, Akima, and shape-preserving splines [14]. The roller coasters’ acceleration, velocity, and displacement data were given in [15]. It is pointed out that in addition to acceleration, it is important to minimize jerk and snap in designing roller coaster paths [16]. The reason for using vertical clothoidal loops instead of circular loops was also discussed for roller coasters [17]. They found that circular loops introduce excess normal forces to the passengers, and a more smooth transition is possible with clothoid curves. For paths in vertical space, another assumption was to minimize the drag work for flying objects. Minimizing the drag force is crucial since energy savings are possible for those paths. The assumption leads to differential equations for which various analytical and numerical results were already presented [18-20].

In this work, assumptions different from those previously mentioned are taken to determine the paths of objects moving in a 2-D vertical space. The  $x$  and  $y$  velocity components are fixed separately, and new differential equations determining the paths are derived for the no net thrust force case and the constant-magnitude thrust force case. The simplest case is the fixed  $x$ -component velocity case with no net thrust force, leading to the well-known parabolic profiles for projectile motions. For the fixed  $y$ -component case, a path that can be described as a ‘2/3 rule’ is found. Depending on the initial inclination angles, peak points are observed in the paths, which shift to the right as the angle ratios decrease. In contrast to the exact analytical solutions for the no thrust force case, the equations are more involved and highly nonlinear for constant-magnitude thrust forces, eliminating the possibility of finding exact analytical solutions. In such cases, approximate analytical solutions are the next best alternative before attempting to solve the equations numerically. Approximate analytical solutions of the equations are found using the Perturbation Iteration Method (PIM) [21,22]. The

method solved Many physical problems with high accuracy [23-26]. Comparisons of the PIM solutions with the adaptive step size Runge-Kutta solutions are outlined. The conditions for which the approximate analytical solutions can replace the numerical solutions are discussed in detail. Generally, the agreement between the analytical and numerical solutions is good for small dimensionless force ratios and initial inclination angles. In contrast, the solutions divert from each other as the force ratios become larger. The results of this work may found applications in determining the paths of flying objects such as projectiles, rockets, and aerial vehicles. Variable thrust force cases, such as incorporating drag forces or other external forces, remain a further area of research. Three-dimensional motions are another potential area of research for fixed velocity component paths.

## 2. MATERIALS AND METHODS

This section will derive the path equations for the no net thrust force case and the net thrust force case using dynamical principles and differential equations.

### 2.1 No Net Thrust Force Case

Consider an object moving in a vertical two-dimensional space with the assumption of no net thrust force parallel to the path, as shown in Figure 1.

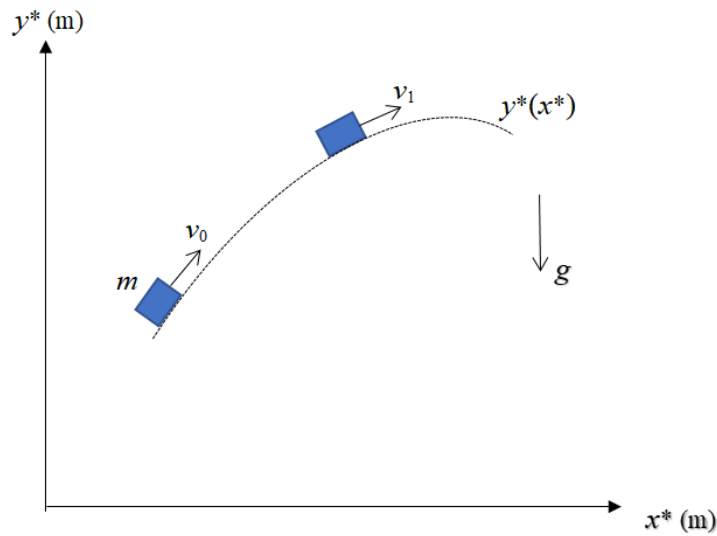


Figure 1. The path of a moving object with no net thrust force

The energy conservation requires are given:

$$\frac{1}{2}mv_0^2 = \frac{1}{2}mv_1^2 + mgy^* \tag{1}$$

The path of the object is  $y^* = y^*(x^*)$ . Decomposing the final velocity into components:

$$v_1^2 = v_{1x}^2 + v_{1y}^2 \tag{2}$$

and bearing in mind that,

$$v_{1y} = y'^* v_{1x} \tag{3}$$

since velocity is always parallel to the path traced, Solving Eqs.(1) - (3) in terms of the velocity components yields,

$$v_{1x} = \sqrt{\frac{v_0^2 - 2gy^*}{1 + y'^*{}^2}} \quad v_{1y} = y' \sqrt{\frac{v_0^2 - 2gy^*}{1 + y'^*{}^2}} \tag{4}$$

#### 2.1.1 Constant x-component velocity

The simplest case is to assume that the  $x$ -component of velocity remains constant during motion. Assuming  $v_{1x} = v_{0x}$ , decomposing the initial velocity  $v_0^2 = v_{0x}^2 + v_{0y}^2$ , solving for  $y'^*$ , from Eq. (4),

$$y'^* = \frac{\sqrt{v_{0y}^2 - 2gy^*}}{v_{0x}} \tag{5}$$

Taking  $y^*(0) = 0$  for the assumption that the starting point is the origin, the equation can be integrated by the separation of variables yielding a solution,

$$y^* = \frac{v_{oy}}{v_{ox}} x^* - \frac{g}{2v_{0x}^2} x^{*2} \tag{6}$$

If the initial slope of the curve is  $y^{*'}(0) = \alpha$ , then,

$$\frac{v_{oy}}{v_{ox}} = \alpha \tag{7}$$

The initial slope turns out to be the ratios of velocity components. The solution can be cast into a dimensionless form by dividing the dimensional coordinates (denoted by an asterisk) by a characteristic length

$$x = \frac{x^*}{L_1} \quad y = \frac{y^*}{L_1} \tag{8}$$

and substituting into Eq. (6), the following equation is obtained,

$$y = \frac{v_{oy}}{v_{ox}} x - \frac{g}{2v_{0x}^2} L_1 x^2 \tag{9}$$

For simplicity, the characteristic length is selected as:

$$L_1 = \frac{v_{0x}^2}{g} \tag{10}$$

and employing Eq. (7), the final dimensionless solution is given by:

$$y = \alpha x - \frac{1}{2} x^2 \tag{11}$$

### 2.1.2 Constant y-component velocity

Assuming  $v_{1y} = v_{oy}$ , decomposing the initial velocity  $v_0^2 = v_{0x}^2 + v_{0y}^2$ , solving for  $y^{*'}$ , from the second equation of Eq. (4),

$$y^{*' } = \frac{v_{oy}}{\sqrt{v_{0x}^2 - 2gy^*}} \tag{12}$$

Integrating the equation and applying the initial condition  $y^*(0) = 0$ , the dimensional solution turns out to be,

$$y^* = \frac{v_{0x}^2}{2g} - \frac{1}{2g^{1/3}} \left( 3v_{oy}x^* - \frac{v_{0x}^3}{g} \right)^{2/3} \tag{13}$$

Using the dimensionless quantities,

$$\frac{v_{oy}}{v_{ox}} = \alpha, \quad x = \frac{x^*}{L_2}, \quad y = \frac{y^*}{L_2} \tag{14}$$

and substituting into Eq. (13),

$$y = \frac{v_{0x}^2}{2gL_2} - \frac{1}{2g^{1/3}L_2} \left( 3v_{oy}L_2x - \frac{v_{0x}^3}{g} \right)^{2/3} \tag{15}$$

For simplicity, the characteristic length is selected as,

$$yL_2 = \frac{v_{0y}^2}{g} \tag{16}$$

The final dimensionless solution is,

$$y = \frac{1}{2} \left[ \frac{1}{\alpha^2} - \left( 3x - \frac{1}{\alpha^3} \right)^{2/3} \right] \tag{17}$$

which depends on the initial inclination as the sole parameter.

## 2.2 Net Thrust Force Case

Consider an object moving in a vertical two-dimensional space with a net thrust force parallel to the path, as shown in Figure 2.

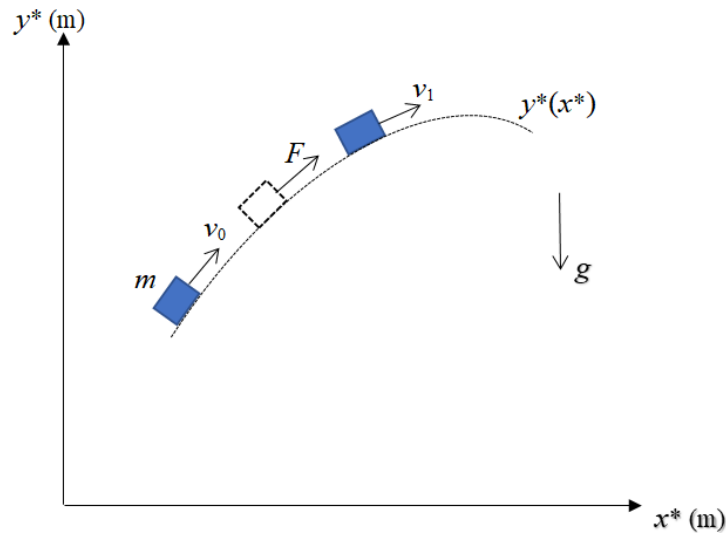


Figure 2. The path of a moving object with thrust force

From the work-energy principle,

$$\frac{1}{2}mv_0^2 + \int_0^s F ds = \frac{1}{2}mv_1^2 + mgy^* \tag{18}$$

where,  $s$  is the curvilinear coordinate along the path. Since the thrust force is constant, it can be taken out of the integral. Using the basic calculus for the length of functions, the integral can be expressed as,  $\int_0^s F ds = \int_0^{x^*} \sqrt{1 + y^{*2}} dx^*$ . Decomposing the final velocity into components, the following equation is obtained:

$$v_1^2 = v_{1x}^2 + v_{1y}^2 \tag{19}$$

and bearing in mind that,

$$v_{1y} = y^{*'} v_{1x} \tag{20}$$

since velocity is always parallel to the path traced. Solving Eqs. (18) - (20) in terms of the velocity components yields,

$$v_{1x} = \sqrt{\frac{v_0^2 + \frac{2F}{m} \int_0^{x^*} \sqrt{1+y^{*2}} dx^* - 2gy^*}{1+y^{*2}}}, \quad v_{1y} = y^{*'} \sqrt{\frac{v_0^2 + \frac{2F}{m} \int_0^{x^*} \sqrt{1+y^{*2}} dx^* - 2gy^*}{1+y^{*2}}} \tag{21}$$

### 2.2.1 Constant x-component velocity

Assume that the  $x$  velocity component remains constant during the motion, namely  $v_{1x} = v_{0x}$ . From the first relation in Eq. (21),

$$v_{0x}^2(1 + y^{*2}) + 2gy^* = v_0^2 + \frac{2F}{m} \int_0^{x^*} \sqrt{1 + y^{*2}} dx^* \tag{22}$$

which is an integro-differential equation. Differentiating the equation once to get rid of the integral, the following equation is obtained:

$$v_{0x}^2 y^{*'} y^{*''} + gy^{*'} - \frac{F}{m} \sqrt{1 + y^{*2}} = 0 \tag{23}$$

Using similar dimensionless quantities as in Section 2.1,

$$x = \frac{x^*}{L_1}, \quad y = \frac{y^*}{L_1}, \quad L_1 = \frac{v_{0x}^2}{g} \tag{24}$$

The differential equation modelling the motion is:

$$y' y'' + y' - \varepsilon \sqrt{1 + y'^2} = 0 \tag{25}$$

where the dimensionless parameter is the ratio of the thrust force to the weight and is given by:

$$\varepsilon = \frac{F}{mg} \tag{26}$$

The conditions are:

$$y(0) = 0, \quad y'(0) = \alpha \tag{27}$$

The exact analytical solution of the problem does not exist. The perturbation iteration method seeks An approximate analytical solution [21,22]. For the nonlinear equation, define

$$F(y', y''; \varepsilon) = y'y'' + y' - \varepsilon\sqrt{1 + y'^2} = 0 \tag{28}$$

A perturbation iteration approximation of a single correction term in the perturbed series is:

$$y_{n+1} = y_n + \varepsilon(y_c)_n, \quad n = 0,1,2, \dots \tag{29}$$

When substituted into Eq. (28) with Taylor expansions of first-order highest derivatives, the following equation is obtained:

$$F(y'_{n+1}, y''_{n+1}; \varepsilon) = F|_{\varepsilon=0} + F_{y'|_{\varepsilon=0}}\varepsilon(y_c)'_n + F_{y''|_{\varepsilon=0}}\varepsilon(y_c)''_n + F_{\varepsilon|_{\varepsilon=0}}\varepsilon \cong 0 \tag{30}$$

yielding finally the equation as:

$$y'_n y''_{n+1} + (1 + y''_n)y'_{n+1} = y'_n y''_n + \varepsilon\sqrt{1 + y_n'^2}, \quad n = 0,1,2, \dots \tag{31}$$

which is the iterative equation for the perturbation iteration algorithm, PIA(1,1). The perturbation iteration method is a systematic way of producing infinitely many algorithms called PIA(*n,m*) where *n* is the number of the correction terms in the perturbation expansions and *m* is the number of highest-order derivatives in the Taylor expansions. PIA(1,1) is the simplest one, having one correction term in the perturbation expansion and first-order derivatives in the Taylor expansion [21,22]. Assume an initial solution,

$$y_0 = \alpha x \tag{32}$$

the next iteration which satisfies the conditions becomes,

$$y_1 = \alpha(\varepsilon\sqrt{1 + \alpha^2} - \alpha)(e^{-x/\alpha} - 1) + \varepsilon\sqrt{1 + \alpha^2}x \tag{33}$$

The second iteration turns out to be a variable coefficient second-order linear equation for which the analytical solution is hard to find. Hence, one terminates at the first iteration.

### 2.2.2 Constant y-component velocity

Assume that the y-component of velocity remains constant during the motion, i.e.,  $v_{1y} = v_{0y}$ . From the second relation in Eq. (21),

$$v_{0y}^2(1 + y^{*2}) = (v_0^2 + \frac{2F}{m} \int_0^{x^*} \sqrt{1 + y^{*2}} dx^* - 2gy^*)y^{*2} \tag{34}$$

or employing the decomposition  $v_0^2 = v_{0x}^2 + v_{0y}^2$  and rearranging,

$$\frac{v_{0y}^2}{y^{*2}} = v_{0x}^2 + \frac{2F}{m} \int_0^{x^*} \sqrt{1 + y^{*2}} dx^* - 2gy^* \tag{35}$$

The above equation is differentiated to eliminate the integral term. The final dimensional equation is:

$$y^{*4} + \frac{F}{mv_{0y}^2} y^{*3} \sqrt{1 + y^{*2}} - \frac{g}{v_{0y}^2} y^{*4} = 0 \tag{36}$$

Using similar dimensionless quantities as in Section 2.2,

$$x = \frac{x^*}{L_2}, \quad y = \frac{y^*}{L_2}, \quad L_2 = \frac{v_{0y}^2}{g} \tag{37}$$

The differential equation determining the dimensionless path curve is:

$$y'' - y'^4 + \varepsilon y'^3 \sqrt{1 + y'^2} = 0 \tag{38}$$

where the dimensionless parameter is the ratio of the thrust force to the weight and is expressed as:

$$\varepsilon = \frac{F}{mg} \tag{39}$$

Using the same initial conditions,

$$y(0) = 0, \quad y'(0) = \alpha \tag{40}$$

Since the exact analytical solution is unavailable, an approximate analytical solution is sought using the perturbation iteration methods [21,22].

For the nonlinear equation

$$F(y', y''; \varepsilon) = y'' - y'^4 + \varepsilon y'^3 \sqrt{1 + y'^2} = 0 \tag{41}$$

A perturbation iteration algorithm, PIA(1,1) approximation given in Eqs. (29) and (30) yields finally the iteration equation:

$$y''_{n+1} - 4y'^3_{n+1} = -y'^3_n (3y'_n + \varepsilon\sqrt{1 + y'^2_n}), \quad n = 0, 1, 2, \dots \tag{42}$$

Assume the trivial solution as the initial solution,

$$y_0 = 0 \tag{43}$$

The two successive iterations yield,

$$y_1 = \alpha x \tag{44}$$

$$y_2 = \frac{\alpha - \varepsilon\sqrt{1 + \alpha^2}}{16\alpha^3} (e^{4\alpha^3 x} - 1) + \frac{3\alpha + \varepsilon\sqrt{1 + \alpha^2}}{4} x \tag{45}$$

Proceeding further requires solutions of variable coefficient non-homogenous second-order linear equations for which the analytical solutions do not exist. Hence, one terminates at the second iteration.

### 3. RESULTS AND DISCUSSION

The numerical results for the path equations are given in this section for both no net thrust force and net thrust force cases.

#### 3.1 No Net Thrust Force Case

The path equations for constant  $x$ -component velocity and constant  $y$ -component velocity were derived in Section 2.1 in the absence of thrust force. Considering the case for constant  $x$ -component velocity, Eq. (11) is the well-known parabolic solution in dimensionless form for the projectile motion, maintaining a constant horizontal component of velocity during motion. In this dimensionless form, the only parameter affecting the paths is the inclination angle (see Figure 3). As the inclination angles increase, the maximum heights are increased with a higher maximum range of motion. One can say that the path maintaining a constant  $y$ -component velocity, i.e. Eq. (17), obeys a special rule of  $2/3$ . Plots of Eq. (17) are given in Figure 4. The peak points of the graphs occur at  $x_m = \frac{1}{3\alpha^3}$  with a maximum value of  $y_m = \frac{1}{2\alpha^2}$ . The nature of the curves (decreasing, increasing) differs at both sides of  $x_m$ . The functions are not differentiable at the peak points since a singularity exists in the first derivative of Eq. (17) at  $x = x_m$ . As the initial inclination angle increases, the peak points decrease and shift to the left.

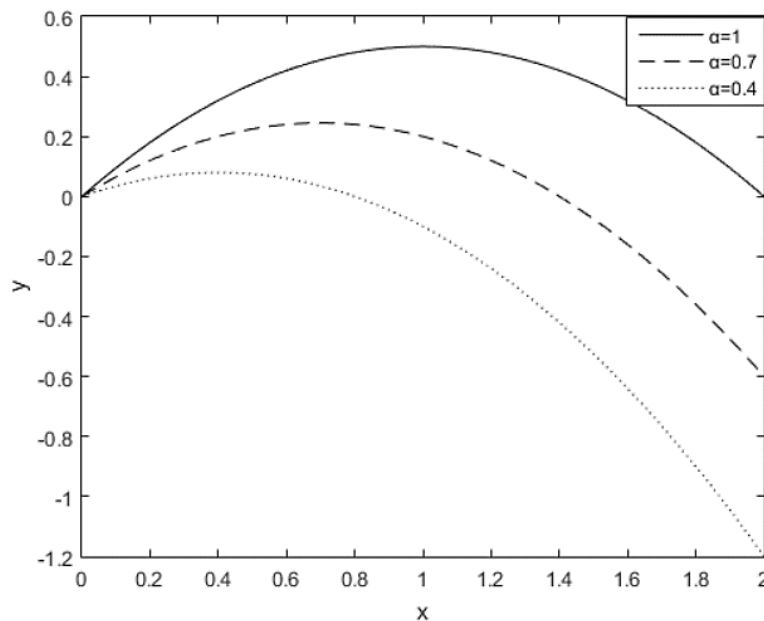


Figure 3. Constant  $x$ -component velocity paths for no thrust force

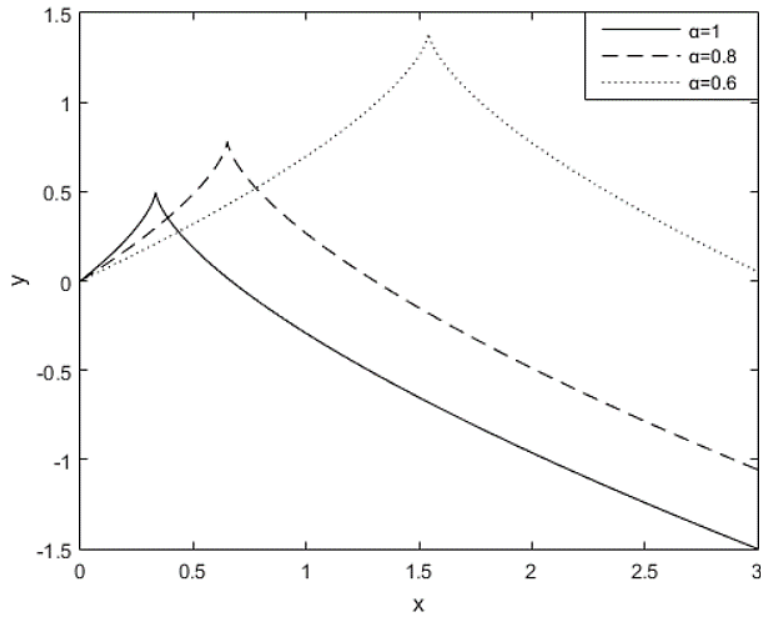


Figure 4. Constant  $y$ -component velocity paths for no thrust force

### 3.2 Net Thrust Force Case

The path equations for constant  $x$ -component velocity and constant  $y$ -component velocity were derived in Section 2.2 when a net thrust force applies to the mass. Considering the case for constant  $x$ -component velocity, the analytical solution given in Eq. (33) is compared with the numerical solutions (see Figure 5). A Matlab algorithm Ordinary Differential Equation (ode45) is used for numerical solutions. For an initial inclination of  $\alpha = 1$ , with the possible exception of very small or large force ratios of  $\varepsilon$ , the analytical solution predicts approximately the constant  $x$ -component paths (see Figure 5). The match is excellent for small force ratios when the inclination angle is small ( $\alpha = 0.2$ ), as seen in Figure 6. When the thrust force to gravity force ratio increases, the solutions start diverging from each other. To ensure close agreement with negligible errors within the domain of interest, it is advised that both the initial inclination angle and the force ratio be kept small compared to 1.

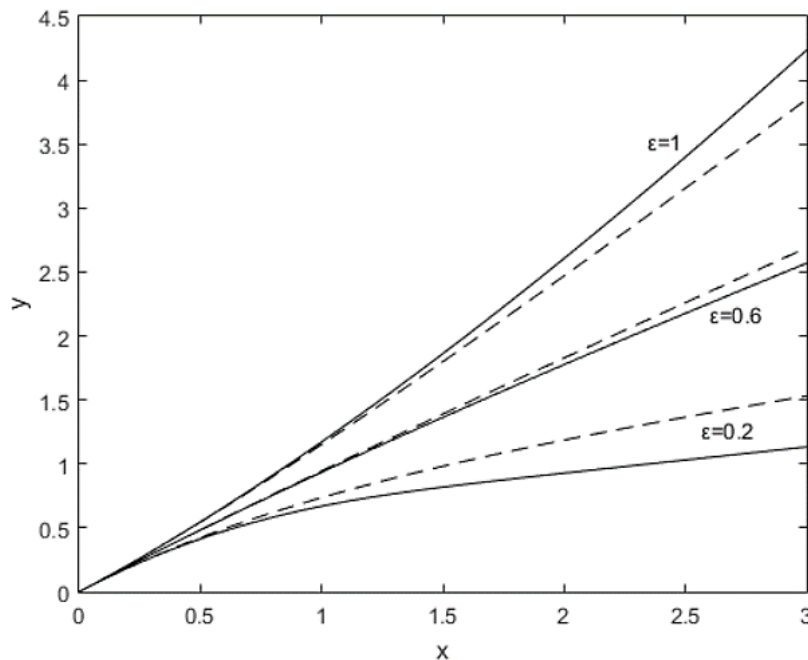


Figure 5. Comparison of numerical (solid) and analytical (dashed) constant  $x$ -component velocity paths for various thrust forces ( $\alpha = 1$ )

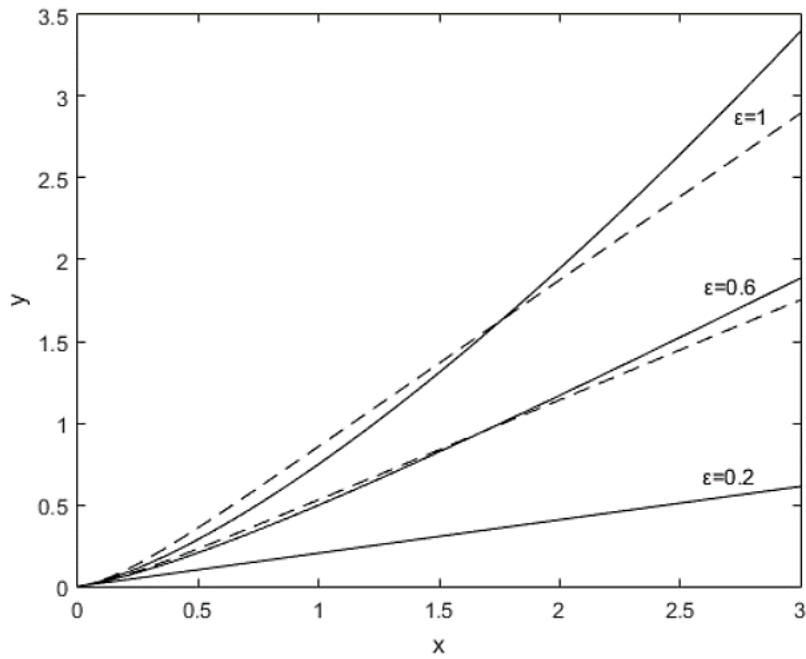


Figure 6. Comparison of numerical (solid) and analytical (dashed) constant  $x$ -component velocity paths for various thrust forces ( $\alpha = 0.2$ )

Considering the case of constant  $y$ -component velocity, the approximate analytical solution in Eq. (45) is compared with the numerical Runge-Kutta solution of the ode45 subroutine from Matlab. For an initial inclination of  $\alpha = 1$ , the analytical and numerical results match each other for small force ratios. Referring to Figure 7, as the force ratio increases, the solutions start diverging from each other. When the inclination angle is smaller ( $\alpha = 0.4$ ), as seen in Figure 8, the match is excellent for small force ratios ( $\varepsilon = 0.4$ ). When the force ratio increases, the solutions start diverging from each other. For small inclination angles, the effects of force ratios are less predominant on the path equations. Generally, if the initial inclination angles and force ratios are not large, the approximate analytical solutions can be replaced with numerical ones. If these dimensionless parameters are large, resorting to numerical solutions would be better for accuracy.

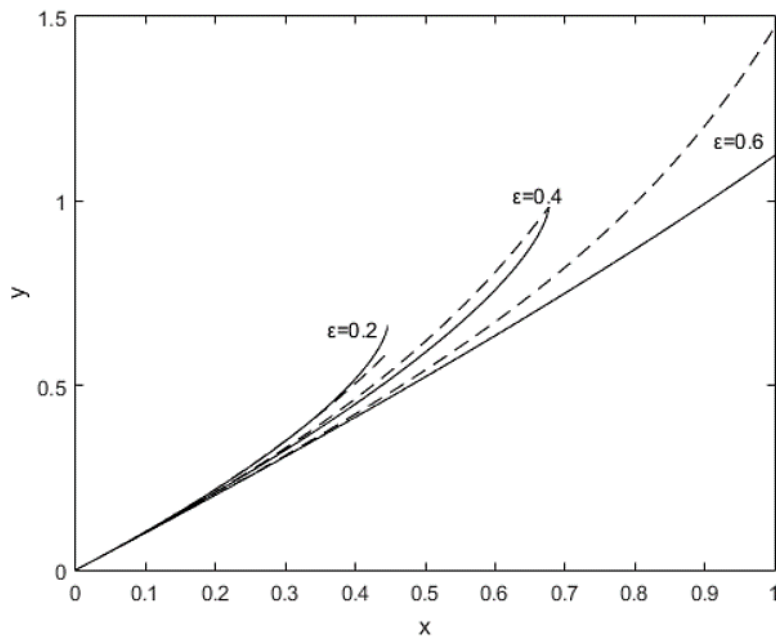


Figure 7. Comparison of numerical (solid) and analytical (dashed) constant  $y$ -component velocity paths for various thrust forces ( $\alpha = 1$ )

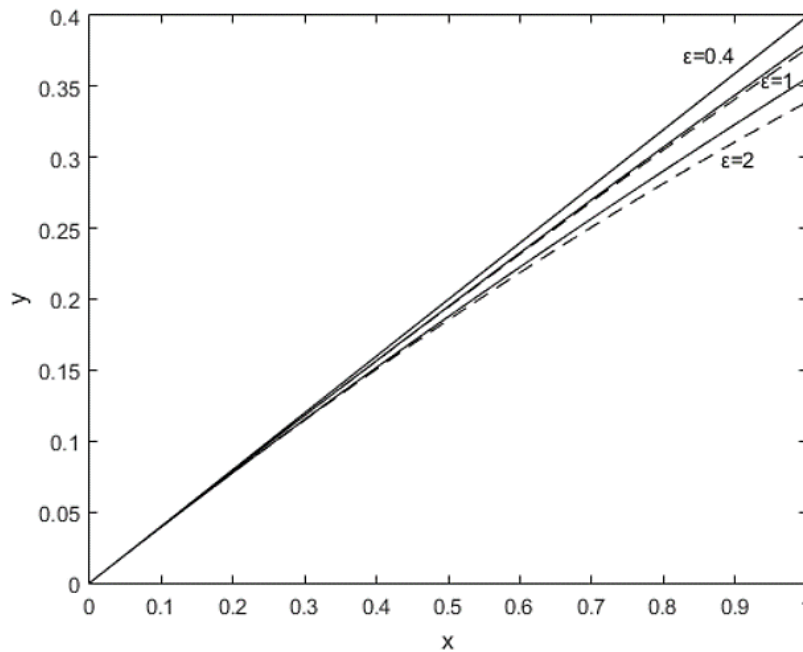


Figure 8. Comparison of numerical (solid) and analytical (dashed) constant  $y$ -component velocity paths for various thrust forces ( $\alpha = 0.4$ )

#### 4. CONCLUSIONS

The differential equations determining the paths are derived for objects moving in a vertical two-dimensional space, assuming that one of the velocity components remains constant during the motion. When no net thrust force is parallel to the motion, the only physical parameter affecting the curves is the initial inclination angle. The differential equations possess exact analytical solutions in terms of this physical parameter. The constant  $x$ -component velocity case leads to the well-known projectile motion with a parabolic solution. In contrast, for the constant  $y$ -component velocity, a so-called special “2/3” rule is proposed. Peak points are observed in the paths which shift to the right as the initial inclination angles decrease. When the thrust force is incorporated into the model, the curves' physical parameters are the initial inclination angle and the dimensionless force ratio. The resulting ordinary differential equations become highly nonlinear without any exact analytical solutions. For such cases, the perturbation-iteration method is employed to construct the approximate analytical solutions. The approximate solutions are compared with the numerical simulations. The analytical solutions can approximate the real solution within the limitations discussed (small inclination angles and force ratios). Dimensionless quantities are used in the analysis for compactness and simplicity of results. The work may find applications in determining paths of aerial vehicles such as projectiles, rockets, airplanes, etc. When ascending or descending, fixing the  $y$ -component of velocity may increase travel comfort for passengers of aerial vehicles. The present study can also be improved by considering three-dimensional motions. Other restrictive velocity/acceleration components or magnitudes of variable thrust forces for paths can also be investigated.

#### ACKNOWLEDGEMENTS

The author thanks Manisa Celal Bayar University, Manisa, Turkey, for their laboratory facilities. The author thanks the anonymous referees and editors for their suggestions on improving the paper. This study was not supported by any grants from funding bodies in the public, private, or not-for-profit sectors.

#### CONFLICT OF INTEREST

The authors declare no conflicts of interest.

#### AUTHORS CONTRIBUTION

M. Pakdemirli (Conceptualization; Formal analysis; Visualisation; Methodology; Data curation; Writing -original draft; Resources)

#### AVAILABILITY OF DATA AND MATERIALS

The data supporting this study's findings are available on request from the corresponding author.

**ETHICS STATEMENT**

Not applicable.

**REFERENCES**

- [1] D. S. Meek, D. J. Walton, "Clothoid spline transition spirals," *Mathematics of Computation*, vol. 59, no. 199, pp. 117-133, 1992.
- [2] M. Shanmugavel, A. Tsourdos, B. White, R. Zbikowski, "Co-operative path planning of multiple UAVs using Dubins paths with clothoid arcs," *Control Engineering Practice*, vol. 18, no. 9, pp. 1084-1092, 2010.
- [3] J. Sanchez-Reyes, J. M. Chacon, "Polynomial approximation to clothoids via s-power series," *Computer Aided Design*, vol. 35, no. 14, pp. 1305-1313, 2003.
- [4] D. S. Meek, D. J. Walton, "An arc spline approximation to a clothoid," *Journal of Computational and Applied Mathematics*, vol. 170, no.1, pp. 59-77, 2004.
- [5] J. McCrae, K. Singh, "Sketching piecewise clothoid curves," *Computers and Graphics*, vol. 33, no. 4, pp. 452-461, 2009.
- [6] M. E. Vázquez-Méndez, G. Casal, J. B. Ferreiro, "Numerical computation of egg and double-egg curves with clothoids," *Journal of Surveying Engineering*, vol. 146, no. 1, p. 04019021, 2019.
- [7] E. Bertolazzi, C. Frego, M. Frego, S. M. Hosseini, A. Peer, "The clothoid: A historical, literary and artistic introduction with applications to technology," in *8th IEEE History of Electrotechnology Conference (HISTELCON)*, pp. 16-19, 2023.
- [8] S. Aashish, S. Southward, M. Ahmadian, "Enhancing autonomous vehicle navigation with a clothoid-based lateral controller," *Applied Sciences*, vol. 14, no. 5, p. 1817, 2024.
- [9] W. Koc, "Identification of transition curves in vehicular roads and railways," *Logistics and Transport*, vol. 28, no. 4, pp. 31-42, 2015.
- [10] P. Woznica, "Optimization of railway entry and exit transition curves," *Open Engineering*, vol. 13, no. 1, p. 20220454, 2023.
- [11] M. Pakdemirli, "Symmetry analysis of the constant acceleration curve equation," *Zeitschrift fur Naturforschung A*, vol. 78, no. 6, pp. 517-524, 2023.
- [12] M. Pakdemirli, V. Yıldız, "Nonlinear curve equations maintaining constant normal accelerations with drag induced tangential decelerations," *Zeitschrift fur Naturforschung A*, vol. 78, no. 2, pp. 125-132, 2023.
- [13] N. M. Sukri, S. M. Nor-Al-Din, N. K. Razali, M. A. A. Mazurin, "Designing roller coaster loops by using extended uniform cubic B-spline," *IOP Conference Series: Materials Science and Engineering*, vol. 1176, no. 1, p. 012039, 2021.
- [14] J. Pombo, "Modeling tracks for roller coaster dynamics," *International Journal of Vehicle Design*, vol. 45, no. 4, pp. 470-499, 2007.
- [15] M. E. Vázquez-Méndez, G. Casal, "The clothoid computation: A simple and efficient numerical algorithm," *Journal of Surveying Engineering*, vol. 142, no. 3, p. 04016005, 2016.
- [16] A-M. Pendrill, D. Eager, "Velocity, acceleration, jerk, snap and vibration: Forces in our bodies during a roller coaster ride," *Physics Education*, vol. 55, no. 6, p. 065012, 2020.
- [17] R. Müller, "Roller coasters without differential equations-A Newtonian approach to constrained motion," *European Journal of Physics*, vol. 31, no. 4, pp. 835-848, 2010.
- [18] M. Pakdemirli, "The drag work minimization path for a flying object with altitude-dependent drag parameters," *Proceedings of the Institution of Mechanical Engineers, Part C, Journal of Mechanical Engineering Science*, vol. 223, no. 5, pp. 1113-1116, 2009.
- [19] E. Yaşar, Y. Yıldırım, "A procedure on the first integrals of second order nonlinear ordinary differential equations," *The European Physical Journal Plus*, vol. 130, pp. 240-244, 2015.
- [20] G. Gün, T. Özer, "First integrals, integrating factors and invariant solutions of the path equation based on Noether and  $\lambda$ -symmetries," *Abstract and Applied Analysis*, vol. 2013, no. 1, p. 284653, 2013.
- [21] Y. Aksoy, M. Pakdemirli, "New perturbation-iteration solutions for Bratu-type equations," *Computers and Mathematics with Applications*, vol. 59, no. 8, pp. 2802-2808, 2010.
- [22] M. Pakdemirli, "Review of the new perturbation-iteration method," *Mathematical and Computational Applications*, vol. 18, no. 3, pp. 139-151, 2013.
- [23] N. Bildik, S. Deniz, "A new efficient method for solving delay differential equations and a comparison with other methods," *The European Physical Journal Plus*, vol. 132, pp. 1-11, 2017.

- [24] M. Şenol, M. Alquran, H. D. Kasmaci, "On the comparison of perturbation-iteration algorithms and residual power series method to solve fractional Zakharov-Kuznetsov equation," *Results in Physics*, vol. 9, pp. 321-327, 2018.
- [25] R. P. Singh, Y. N. Reddy, "Perturbation iteration method for solving differential difference equations having boundary layer," *Communications in Mathematics and Applications*, vol. 11, no. 4, pp. 617-633, 2020.
- [26] H. M. Srivastava, S. Deniz, K. M. Saad, "An efficient semi-analytical method for solving the generalized regularized long wave equations with a new fractional derivative operator," *Journal of King Saud University-Science*, vol. 33, p. 101345, 2021.

## NOMENCLATURE

$x^*$	dimensional horizontal coordinate (m)	$\alpha$	initial slope of the curve (unitless)
$y^*$	dimensional vertical coordinate (m)	$L_1$	characteristic length used for nondimensionalization (m)
$x$	dimensionless horizontal coordinate (unitless)	$L_2$	characteristic length used for nondimensionalization (m)
$y$	dimensionless vertical coordinate (unitless)	$F$	thrust force (N)
$m$	mass (kg)	$s$	curvilinear coordinate along the path (m)
$g$	gravitational acceleration ( $m/s^2$ )	$\varepsilon$	ratio of the thrust force to the weight (unitless)
$v_0$	initial velocity (m/s)	$y_n$	$n$ 'th iteration solution (unitless)
$v_1$	final velocity (m/s)	$(y_c)_n$	correction to the $n$ 'th iteration solution (unitless)
$v_{1x}$	$x$ component of final velocity (m/s)	$y_{n+1}$	$n+1$ 'th iteration solution (unitless)
$v_{1y}$	$y$ component of final velocity (m/s)		